

Research article

IN-SILICO DESIGN AND SCREENING OF QUINOLONE DERIVATIVES AGAINST GYRASE OF STAPHYLOCOCCUS AUREUS

**Ronjano Kikon¹, Dipak Chetia¹, Malita Sarma Borthakur¹, Lima Patowary^{1,2},
Dubom Tayeng¹, James H. Zothantluanga^{1*}**

¹Department of Pharmaceutical Sciences, Faculty of Science and Engineering, Dibrugarh University, Dibrugarh 786004, Assam, India

²Department of Pharmaceutical Chemistry, Girijananda Chowdhury Institute of Pharmaceutical Science, Guwahati 781017, Assam, India

Abstract

Background: *The healthcare sector is facing an unprecedented amount of pressure due to antibiotic resistance. This problem mandates the need for newer molecules with higher efficacy and lower toxicity.*

Objective: *In this study, we aim to virtually design and carry out in-silico studies to identify a potent quinolone derivative by targeting Staphylococcus aureus gyrase (SaG).*

Methods: *Data Warrior software, Discovery studio software, Molinspiration Chemoinformatics web tool, Swiss ADME web tool, and ProTox-II web tool were used to study the quinolone derivatives.*

Results and Discussion: *Initially, 21 quinolone derivatives were preliminarily screened for their toxicity and ADME. Among the quinolone derivatives that passed the preliminary testing, C15 was found as the best drug-like molecule. C15 has a good binding affinity (-20.1599 kcal/mol) to the active binding site of SaG. C15 also showed similar protein-ligand interactions (ARG B:1122) with SaG native ligand (RXV1021) and the original quinolone moiety (C1). C15 was predicted to have a moderate biological activity with a high bioavailability score. The LD₅₀ of C15 was computed to be 2500 mg/kg bodyweight. C15 showed negative results in tests for carcinogenicity, immunotoxicity, mutagenicity, and cytotoxicity with a 51% chance of being hepatotoxic.*

Conclusion: *We conclude that the C15 derivative containing iodine in the 5th position is the most potent quinolone derivative for potentially inhibiting S. aureus by binding to the gyrase protein. We recommend synthesis with subsequent evaluation of in-vitro antibacterial activity to confirm the in-silico potency observed in this study.*

*Corresponding author's E-mail: jameshzta@gmail.com

Keywords: *In-silico*; Quinolone; Antibiotics; Drug resistance; *Staphylococcus aureus*

Introduction

Antibiotics are bacteria-targeting chemicals that are used to treat and prevent bacterial illnesses and are widely utilized in modern medicine[1]. Selman Waksman coined the term "antibiotic" to describe any tiny molecule produced by a bacteria that inhibit the growth of other microbes[2,3]. For thousands of years, infectious diseases were a major cause of mortality often leading to epidemic proportions and killing millions of people[3,4]. For a very long time, efforts to combat, treat, and stop the spread of contagious diseases were fruitless given the lack of information[3]. Sir Alexander Fleming (1881-1955) discovered penicillin in 1928, which kicked off the antibiotic revolution leading to the "Golden Age of Novel Antibiotic Discovery" from the 1950s to the 1970s. No other antibiotic classes have been discovered since then[4].

Antibiotics have been a source of life for many decades. The gradual increase in resistance to most antibiotics drugs has become a worldwide problem. Antibiotics disrupt the composition of the infectious agent, leading to bacterial adaptation or mutations, and in turn, to new strains that are resistant to the current antibiotic regimen[5]. Many antibiotics' effectiveness is declining at an alarming rate, as bacteria become highly resistant to the present supply of antibiotics. This is primarily due to natural evolution, but it is also owing to almost 80 years of irresponsible use[6]. The inappropriate use of antibiotics in one patient might develop a resistant strain that spreads to other patients that do not use antibiotics, which makes this issue a pressing public health problem. Bacterial adaptation leads to the formation of new antibiotic-resistant strains which may neutralize an antibiotic by altering its component to render it ineffective[5]. Resistance normally develops two to three years following the launch of a new antibiotic medication. Finding innovative, active molecules with the desired properties for use as antibiotics has become increasingly difficult[6].

Due to failure in various rounds of clinical trials, there has recently been a drop in the number of new antibiotics on the market[7]. To address this issue, a multisectoral and interdisciplinary approach is required, as well as coordinated efforts [8]. The fundamental issue with antibiotic treatment is that if a new antibiotic is introduced, resistance to it will develop sooner or later. We must learn to target pathogens with more precision and restrict the indiscriminate use of antimicrobials

and other activities that hasten the establishment of emerging resistance mechanisms[9].

Quinolone class of antibiotics are broad-spectrum antibiotics that work against Gram-positive and Gram-negative bacteria, as well as anaerobes and mycobacteria[10]. Quinolones are bactericidal chemotherapeutics that prevent bacterial DNA replication and transcription by prohibiting bacterial DNA from unwinding and duplicating, interfering with DNA replication, and resulting in cell death[11,12]. The quinolone class of antibacterial medicines has a long history of use in the treatment of bacterial infections. Their bactericidal capabilities and unique method of action make them appealing medicinal agents[13].

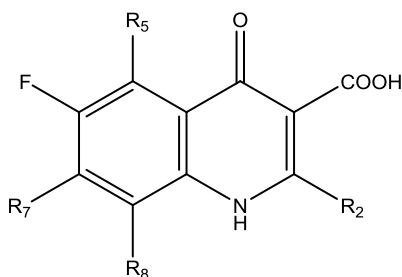


Figure 1 The nucleus of quinolone antibiotics

Quinolone antibiotics have a quinolone core with an N-linked cyclic moiety and different substituents at the C(6) and/or C(7) locations. In quinolone structure, there are 6 important positions for modifications to improve the activity of the drug: R1, R5, R6, R7, R8, and X. X = C defines quinolones, and X = N defines naphthyridines[10]. Substitution at the R2 position decreases the activity of the group. At the R6 position, if we substituted the Hydrogen with Fluorine, it will increase the activity of the group. All quinolones in use contain fluoroquinolone in their chemical structure and thus they are referred to as Fluoroquinolone. N₁ substitution is necessary for its activity. Small Alkyl groups or cycloalkyl groups increase it[10,14]. In the present study, we will design quinolone derivatives and carry out *in-silico* studies to screen their potential biological activity against *Staphylococcus aureus* gyrase (SaG).

Materials and Methods

Hardware

Molecular modeling studies were carried out with the Dell Precision Tower work station 3620 running Intel i7 7th generation octa-core Processor, 2 TB hard disk, 16 GB RAM, and NVidia Quadro K420 graphics card.

Ligand Preparation

The Ligands are saved together in a single file. The ligand file was loaded into DS 2020 and prepared to generate their 3D conformations. After preparation, energy minimizations of the ligands were done with the smart minimizer algorithm tool of DS 2020.

Processing of protein

The 2.1 Å (resolution) crystal structure of the *SaG* complex with GSK299423 and DNA which has a Protein Data Bank (PDB) ID of 2XCS was retrieved from the PDB Website (<https://www.rcsb.org>). It was saved in the .pdb file format. Biovia Discovery Studio 2020 (DS 2020) was used to pre-process the target protein. At first, the water molecules, hetero atoms, coenzymes present along with the protein, and all other side chains except chain A were eliminated. Following this, hydrogen was added to the protein. After this, the protein was saved in the .sdf format. The energy of the prepared protein is minimized with the smart minimizer algorithm of DS 2020. The active binding site of the target protein was determined with the 'Define and Edit Binding Sites' tool of DS 2020 around the co-crystal ligand. The coordinates of the Binding Sites were also determined with the 'Attributes of SBD Side Sphere' option of DS2020. The XYZ coordinates of the active binding site are $x = 6.33$, $y = 44.39$, $z = 40.20$ with a radius of 11.4 Å.

Molecular docking simulation studies (MDSS)

After the active binding site was identified, we proceed with the MDSS of the ligands with the target protein. Docking was done with the C-Docker Protocol from DS 2020. Analysis of ligand interactions was also carried out with the DS visualizer.

Miscellaneous

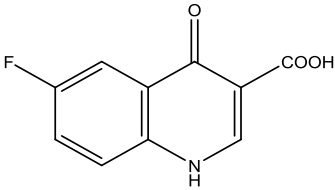
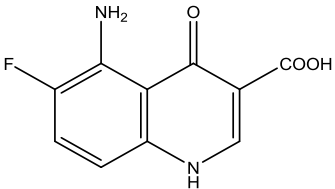
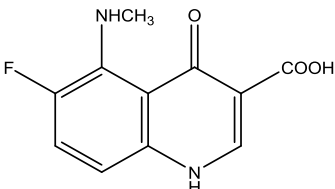
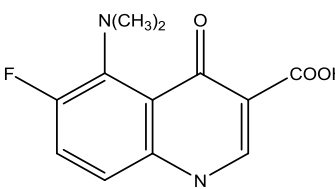
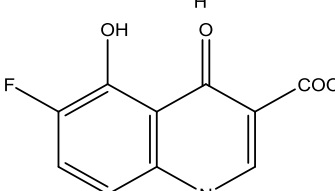
The biological activity of C15 was predicted with the Molinspiration Chemoinformatics web tool (<https://www.molinspiration.com>). An in-depth analysis of C15 was carried out with the SwissADME web tool [15]. Toxicity studies on C15 were further carried out with the ProTox-II web tool [16].

Results and Discussion

Design of quinolone derivatives

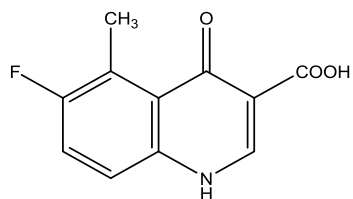
Modifications were made at the C5 position of the quinolone nucleus. A total of 21 quinolone derivatives were prepared. Their 2D chemical structures along with their respective compound code are listed in Table 1. The SMILES ID of all the compounds was generated with the Chem Draw Professionals 16.0 software.

Table 1 List of quinolone derivatives

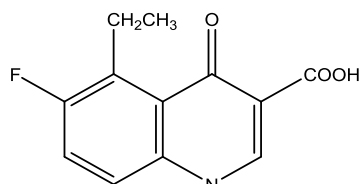
Compound code	Chemical structure
C1 (original)	
C2	
C3	
C4	
C5	

Design and screening of quinoline derivatives

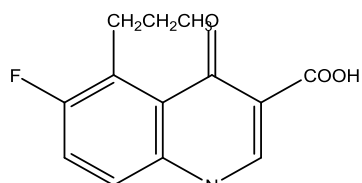
C6



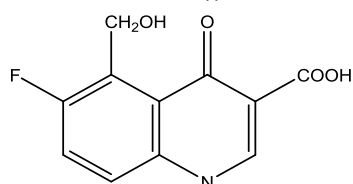
C7



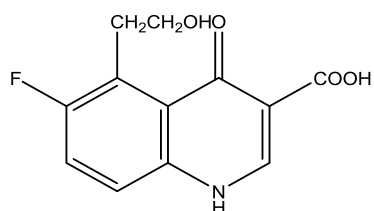
C8



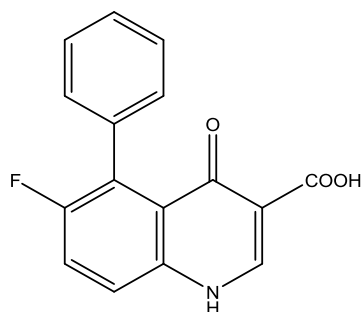
C9



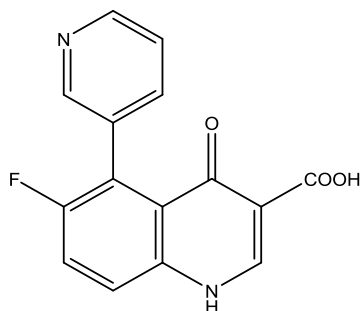
C10



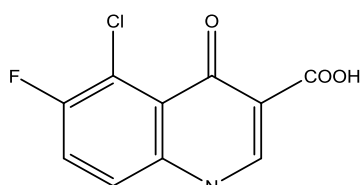
C11



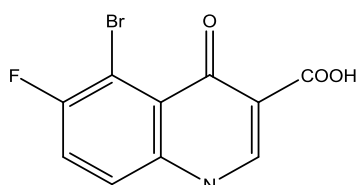
C12



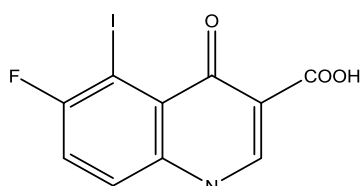
C13



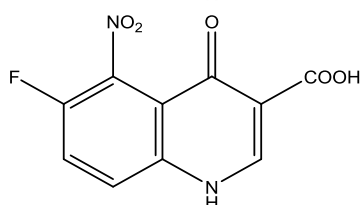
C14



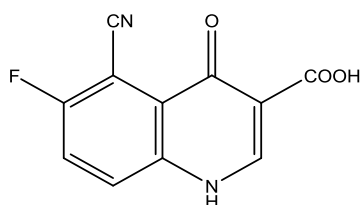
C15



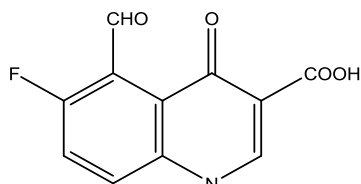
C16



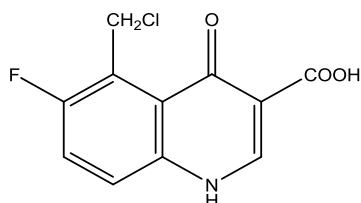
C17



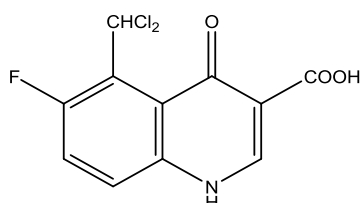
C18



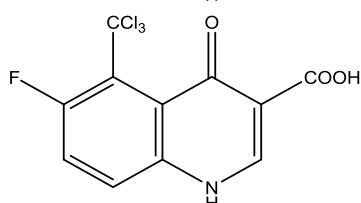
C19



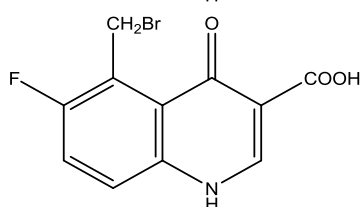
C20



C21



C22



Preliminary toxicity studies with Data Warrior software

Toxicity often leads to the prevention or withdrawal of drugs from clinical use [17]. For the next step in designing quinolone derivatives, we carried out *in-silico* toxicity studies with the Data Warrior software. Data Warrior is a reliable software used by many researchers [18–20]. The results of the toxicity analysis of the quinolone derivatives are given in Table 2. According to the study, C11, C19, C20, C21, and C22 showed signs of toxicity. Therefore, these five compounds were discarded from the study.

Table 2 Toxicity analysis of 22 quinolone derivatives

Code	Mutagenic	Tumorigenic	Reproductive effective	Irritant
C1 (original)	none	none	none	none
C2	none	none	none	none
C3	none	none	none	none
C4	none	none	none	none
C5	none	none	none	none
C6	none	none	none	none
C7	none	none	none	none
C8	none	none	none	none
C9	none	none	none	none
C10	none	none	none	none
C11	none	none	none	high
C12	none	none	none	none
C13	none	none	none	none
C14	none	none	none	none
C15	none	none	none	none
C16	none	none	none	none
C17	none	none	none	none
C18	none	none	none	none
C19	high	high	high	none
C20	high	high	high	high
C21	high	high	high	high
C22	high	high	high	none

Preliminary ADME studies with Lipinski's rule

Compounds that are active under *in-vitro* settings can show lower activity under *in-vivo* conditions due to poor ADME properties. Therefore, in addition to toxicity, bioavailability is another important issue that needs to be addressed [20,21]. Lipinski criteria are a set of flexible guidelines that determine the possibility of oral bioavailability and "drug-like" properties in a substance. Lipinski's rule of Five or simply the rule of five (RO5) is a rule of thumb to evaluate drug-likeness or to determine if a chemical compound with a certain pharmacological or biological activity has chemical properties and physical properties that would make it a likely orally active drug in humans [22]. Lipinski considers the following parameters to estimate the bioavailability of compounds:

1. Not more than 5 Hydrogen bond donors
2. Not more than 10 Hydrogen bond acceptors
3. molecular mass less than 500 Daltons

4. $\text{Log}P_{\text{OW}}$ partition coefficient does not exceed 5

The ADME properties of the quinolone derivatives are given in Table 3. All the compounds corroborate to specified parameters of Lipinski's rule of 5. It is assumed that they will most likely be bioavailable. Therefore, quinolone derivatives that were free from toxicity and bioavailability issues were subjected to further studies.

Table 3 Evaluation of quinolone derivatives against Lipinski's rule of 5

Molecule Name	Mol weight	cLogP	cLogS	H-Acceptors	H-Donors	Lipinski violations
C1 (Original)	207.16	0.1235	-2.613	4	2	0
C2	222.175	-0.5538	-2.689	5	3	0
C3	236.201	-0.2295	-2.673	5	3	0
C4	250.228	0.0199	-2.649	5	2	0
C5	223.159	-0.2222	-2.317	5	3	0
C6	221.187	0.4674	-2.957	4	2	0
C7	235.213	0.883	-3.116	4	2	0
C8	249.24	1.3374	-3.386	4	2	0
C9	237.186	-0.4738	-2.497	5	3	0
C10	251.212	-0.0437	-2.609	5	3	0
C12	284.245	0.7818	-3.904	5	2	0
C13	241.605	0.7295	-3.349	4	2	0
C14	286.056	0.8487	-3.447	4	2	0
C15	333.052	0.5606	-3.629	4	2	0
C16	252.157	-0.7981	-3.073	7	2	0
C17	232.17	-0.0409	-3.386	5	2	0
C18	235.17	0.0568	-2.937	5	2	0

Molecular docking simulation studies

MDSS is a simple and effective technique for studying the ligand binding affinity, binding pose, and interaction with a protein [23–27]. MDSS was carried out to study the binding affinity, binding pose, and ligand interactions of quinolone derivatives towards the active binding site of SaG. The X-ray crystal structure of SaG is given in Figure 2. Lower binding energy indicates a better binding affinity [28]. In our study, the binding energy of the native ligand (RXV1021) and the original compound (C1) will be used as a benchmark to judge the binding affinity of the quinolone derivatives. The binding energy of all the compounds is given in Table 4. After comparing the binding energy of the compounds with the original

(C1) and Standard (RXV1021), 4 compounds (C7, C8, C9, C15) showed lower binding energy (higher binding affinity) towards the active binding site of the *SaG*.

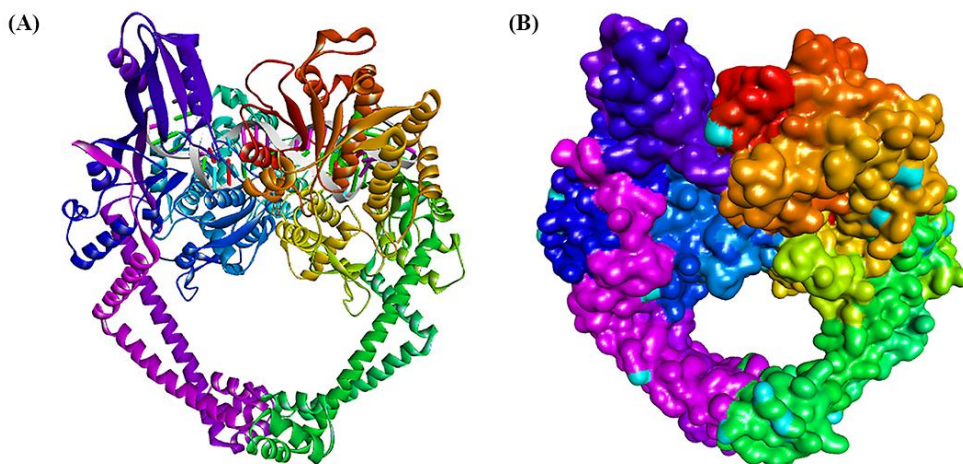


Figure 2 X-ray crystal structure of the (A) 2D and (B) 3D images of *SaG*.

Table 4 Binding energies of quinolone derivatives

Code	Cdocking energy (kcal/mol)
C1 (Original)	-20.0426
C2	-17.0103
C3	-15.9448
C4	-18.5208
C5	-18.0235
C6	-17.2653
C7	-20.1786
C8	-22.0135
C9	-20.8492
C10	-18.6499
C12	-10.7813
C13	-14.5586
C14	-15.4169
C15	-20.1599
C16	-14.4019
C17	-18.1682
C18	-19.9695
RXV1021	-1.72064

Analysis of protein-ligand interactions

When we carried out a preliminary observation of the protein-ligand interactions, we observe that C8 did not form any conventional hydrogen bond. Also, C1 (-1.1237), C7 (-1.3235), and C9 (-1.1918) were computed to have a lower drug-likeness value when compared to C15 (-0.5595) (results generated from Data Warrior software). Therefore, we decided to observe the protein-ligand interaction of only C15 as it was computed to be the most drug-like molecule among the entire quinolone derivatives. The 2D protein-ligand interactions of the native ligand, a quinolone (C1), and quinolone derivative (C15) are given in Figure 3. The native ligand and C15 shared similar hydrophobic interactions with DG F:10, DG E:10, and DC E:11. The native ligand interacted with ARG B:1122 of sub-unit B while C15 interacted with ARG D:1122 of sub-unit D through conventional hydrogen bonds, respectively. Also, C1 and C15 shared similar interactions with ARG D:1122 (conventional hydrogen bond).

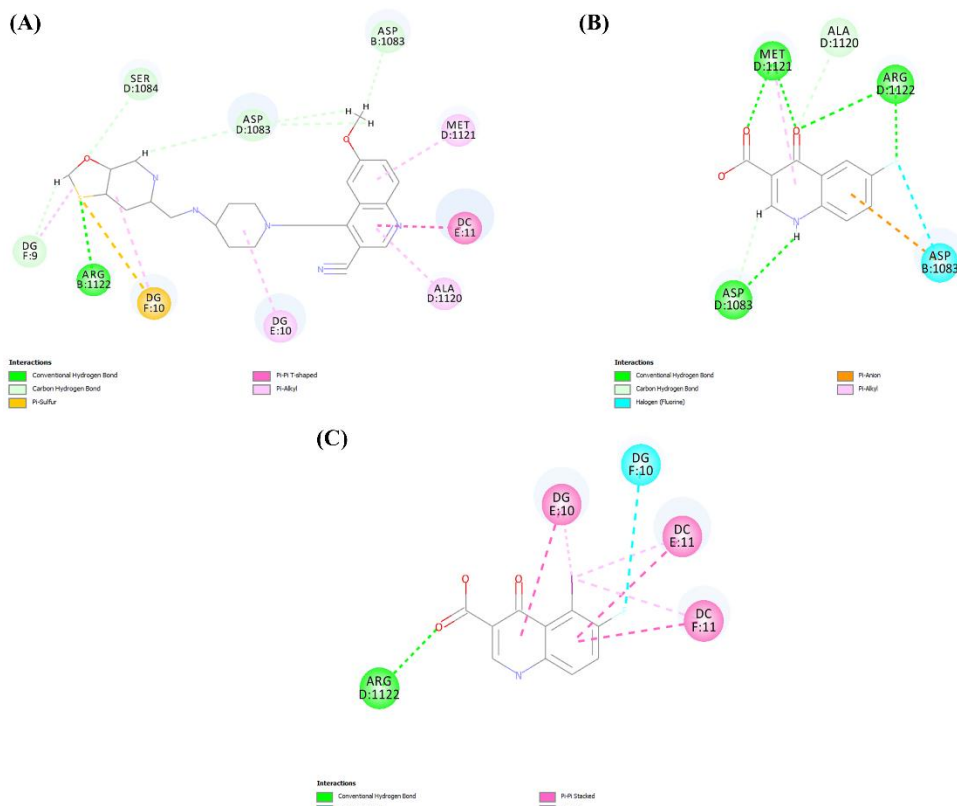


Figure 3 Graphical representation of the 2D protein-ligand interactions of (A) native ligand, (B) quinolone (C1), and (C) quinolone derivative (C15) with the amino acids present at the active binding site of the *SaG*.

Biological activity prediction of C15

The biological activity of C15 was predicted with the Molinspiration Chemoinformatics web tool. The results of the predicted biological activity are given in Table 5. The score ranges from -3 (bad activity) to +3 (good activity). Based on this prediction, C15 was considered to possess a moderate biological activity.

Table 5 Predicted biological activity of C15

Activity	Score
GPCR ligand	-0.32
Ion channel modulator	0.00
Kinase inhibitor	-0.24
Nuclear receptor ligand	-0.32
Protease inhibitor	-0.72
Enzyme inhibitor	0.02

Detailed ADME analysis of C15

The bioavailability of C15 was evaluated with the BOILED-EGG model (Figure 4). From the BOILED Egg model, we can see that C15 will be able to penetrate the blood-brain barrier. C15 will also be easily absorbed from the gastrointestinal tract. Also, C15 will not be removed from the cells due to the action of p-glycoproteins. Upon observing the pharmacokinetics of C15, we observe that it will not interact with any of the hepatic enzymes (CYP1A2, CYP2C19, CYP2C9, CYP2D6, and CYP3A4). Also, in addition to Lipinski's rule, C15 does not violate the Ghose filter, Veber filter, Egan filter, and Muegge filter [29–32]. The bioavailability score of C15 was computed to be 0.85 (maximum score = 1). C15 was also computed to have a lead-like property. The synthetic accessibility score of C15 was 2.02 which means that the synthesis of C15 will most likely be easy [33].

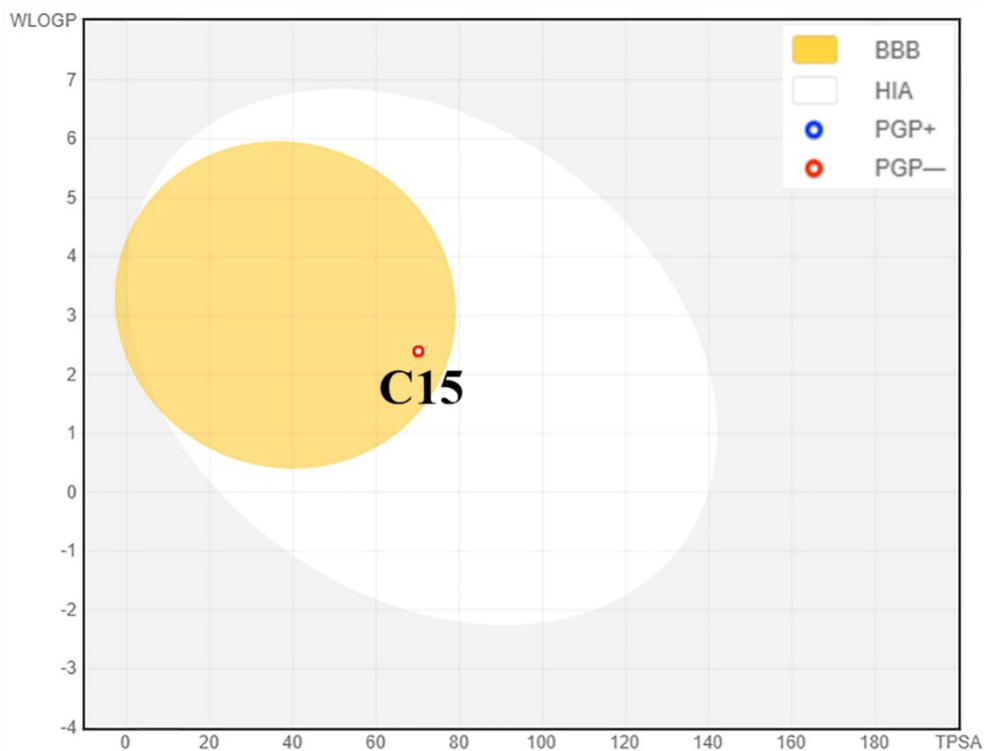


Figure 4 BOILED Egg model of C15

Additional toxicity analysis of C15

Additional toxicity analysis of C15 was carried out with the ProTox-II web server [16]. The median lethal dose (LD_{50}) of C15, the toxicity class, and other toxicity endpoints were computed. The LD_{50} of C15 was computed to be 2500 mg/kg bodyweight. C15 was predicted to belong to the toxicity class of 5. Class 5 toxicity suggests that C15 might be harmful if swallowed ($2000 < LD_{50} \leq 5000$). C15 showed negative results in the tests for carcinogenicity, immunotoxicity, mutagenicity, and cytotoxicity. However, there is a 51% chance that C15 might be toxic to hepatic cells. The overall prediction accuracy for the LD_{50} , toxicity class, and toxicity endpoints was 67.38%.

Conclusion

Improper use of antibiotics and gene transfer among different bacteria species are the main cause leading to the increase in the rate of antibiotic resistance among bacterial species. After analyzing all parameters, including ADME properties, toxicity data, binding energy, and drug-likeness, C15 was identified as the derivative with potential inhibitory activity against *SaG*. C15 contains 'Iodine (I)' in the 5th

position. In the future, C15 can be synthesized and examined for its *in-vitro* activity to confirm the *in-silico* antibacterial potency displayed in the study.

Conflict of Interest

The authors declare no conflicting interests.

Funding

Not applicable.

References

1. Calhoun C, Wermuth HR, Hall GA. Antibiotics. StatPearls. 2022.
2. Ribeiro da Cunha, Fonseca, Calado. Antibiotic Discovery: Where Have We Come from, Where Do We Go? Antibiotics 2019; 8:45.
3. Mohr KI. History of Antibiotics Research. In 2016. p. 237–72.
4. Adedeji WA. The treasure called antibiotics. Ann Ibadan Postgrad Med 2016; 14:56–7.
5. Habboush Y, Guzman N. Antibiotic Resistance. StatPearls. 2022.
6. Dutescu IA, Hillier SA. Encouraging the Development of New Antibiotics: Are Financial Incentives the Right Way Forward? A Systematic Review and Case Study. Infect Drug Resist 2021; 14:415–34.
7. Batool M, Ahmad B, Choi S. A Structure-Based Drug Discovery Paradigm. Int J Mol Sci 2019; 20:2783.
8. Shlaes DM, Bradford PA. Antibiotics—From There to Where? Pathog Immun 2018; 3:19.
9. Aminov RI. A Brief History of the Antibiotic Era: Lessons Learned and Challenges for the Future. Front Microbiol 2010; 1.
10. Pham TDM, Ziora ZM, Blaskovich MAT. Quinolone antibiotics. Medchemcomm 2019; 10:1719–39.
11. Hooper D. Emerging Mechanisms of Fluoroquinolone Resistance. Emerg Infect Dis 2001; 7:337–41.
12. Uivarosi V. Metal Complexes of Quinolone Antibiotics and Their Applications: An Update. Molecules 2013; 18:11153–97.
13. Wiles JA, Bradbury BJ, Pucci MJ. New quinolone antibiotics: a survey of the literature from 2005 to 2010. Expert Opin Ther Pat 2010; 20:1295–319.
14. Briguglio I, Piras S, Corona P, Pirisi M, Jabes D, Carta A. SAR and Anti-Mycobacterial Activity of Quinolones and Triazoloquinolones: An Update. Anti-Infective Agents 2012; 11:75–89.
15. Daina A, Michielin O, Zoete V. SwissADME: a free web tool to evaluate pharmacokinetics, drug-likeness and medicinal chemistry friendliness of

- small molecules. *Sci Rep* 2017; 7:42717.
16. Banerjee P, Eckert AO, Schrey AK, Preissner R. ProTox-II: a webserver for the prediction of toxicity of chemicals. *Nucleic Acids Res* 2018; 46:W257–63.
 17. Antimalarial Flavonoid-Glycoside from *Acacia pennata* with Inhibitory Potential Against PfDHFR-TS: An In-silico Study. *Biointerface Res Appl Chem* 2021; 12:4871–87.
 18. Patowary L, Borthakur MS, Zothantluanga JH, Chetia D. Repurposing of FDA approved drugs having structural similarity to artemisinin against PfDHFR-TS through molecular docking and molecular dynamics simulation studies. *Curr Trends Pharm Res* 2021; 8:14–34.
 19. Zothantluanga JH, Gogoi N, Shakya A, Chetia D, Lalthanzara H. Computational guided identification of potential leads from *Acacia pennata* (L.) Willd. as inhibitors for cellular entry and viral replication of SARS-CoV-2. *Futur J Pharm Sci* 2021; 7:201.
 20. Zothantluanga JH. Molecular Docking Simulation Studies, Toxicity Study, Bioactivity Prediction, and Structure-Activity Relationship Reveals Rutin as a Potential Inhibitor of SARS-CoV-2 3CL pro. *J Sci Res* 2021; 65:96–104.
 21. Paul S, Hmar EBL, Zothantluanga JH, Sharma HK. Essential oils: a review on their salient biological activities and major delivery strategies. *Sci Vis* 2020; 20:54–71.
 22. McKerrow JH, Lipinski CA. The rule of five should not impede anti-parasitic drug development. *Int J Parasitol Drugs Drug Resist* 2017; 7:248–9.
 23. Umar AK, Kelutur FJ, Zothantluanga JH. Flavonoid Compounds of Buah Merah (*Pandanus conoideus* Lamk) as a Potent Oxidative Stress Modulator in ROS-induced Cancer: In Silico Approach. *Maj Obat Tradis* 2021; 26:221.
 24. Umar AK, Zothantluanga JH. Structure-Based Virtual Screening and Molecular Dynamics of Quercetin and Its Natural Derivatives as Potent Oxidative Stress Modulators in ROS-induced Cancer. *Indones J Pharm* 2021; 3:60.
 25. Pasala PK, Abbas Shaik R, Rudrapal M, Khan J, Alaidarous MA, Jagdish Khairnar S, et al. Cerebroprotective effect of Aloe Emodin: In silico and in vivo studies. *Saudi J Biol Sci* 2022; 29:998–1005.
 26. Pasala PK, Uppara RK, Rudrapal M, Zothantluanga JH, Umar AK. Silybin phytosome attenuates cerebral ischemia-reperfusion injury in rats by suppressing oxidative stress and reducing inflammatory response: In vivo and in silico approaches. *J Biochem Mol Toxicol* 2022.<http://dx.doi.org/10.1002/jbt.23073>.
 27. Rudrapal M, Celik I, Khan J, Ansari MA, Alomary MN, Yadav R, et al. Identification of bioactive molecules from *Triphala* (Ayurvedic herbal

- formulation) as potential inhibitors of SARS-CoV-2 main protease (Mpro) through computational investigations. *J King Saud Univ - Sci* 2022; 34:101826.
28. Zothantluanga JH, Abdalla M, Rudrapal M, Tian Q, Chetia D, Li J. Computational Investigations for Identification of Bioactive Molecules from *Baccaurea ramiflora* and *Bergenia ciliata* as Inhibitors of SARS-CoV-2 M pro. *Polycycl Aromat Compd* 2022; 1–29.
 29. Ghose AK, Viswanadhan VN, Wendoloski JJ. A knowledge-based approach in designing combinatorial or medicinal chemistry libraries for drug discovery. 1. A qualitative and quantitative characterization of known drug databases. *J Comb Chem* 1999; 1:55–68.
 30. Veber DF, Johnson SR, Cheng H-Y, Smith BR, Ward KW, Kopple KD. Molecular Properties That Influence the Oral Bioavailability of Drug Candidates. *J Med Chem* 2002; 45:2615–23.
 31. Egan WJ, Merz, KM, Baldwin JJ. Prediction of Drug Absorption Using Multivariate Statistics. *J Med Chem* 2000; 43:3867–77.
 32. Muegge I, Heald SL, Brittelli D. Simple Selection Criteria for Drug-like Chemical Matter. *J Med Chem* 2001; 44:1841–6.
 33. Umar AK, Zothantluanga JH, Aswin K, Maulana S, Sulaiman Zubair M, Lahlhenmawia H, et al. Antiviral phytocompounds “ellagic acid” and “(+)-sesamin” of *Bridelia retusa* identified as potential inhibitors of SARS-CoV-2 3CL pro using extensive molecular docking, molecular dynamics simulation studies, binding free energy calculations, and bioactivi. *Struct Chem* 2022; 33:1-21.

How to cite this article:

Kikon R, Chetia D, Borthakur MS, Patowary L, Tayeng D, Zothantluanga JH. *In-silico* design and screening of quinolone derivatives against gyrase of *Staphylococcus aureus*, *Curr Trends Pharm Res*, 2022;9 (1): 1-16.